

An ErbB3 Antibody, MM-121, Is Active in Cancers with Ligand-Dependent Activation

Birgit Schoeberl¹, Anthony C. Faber², Danan Li^{3,4}, Mei-Chih Liang^{3,4}, Katherine Crosby⁶, Matthew Onsum¹, Olga Burenkova¹, Emily Pace¹, Zandra Walton^{3,4}, Lin Nie¹, Aaron Fulgham¹, Youngchul Song², Ulrik B. Nielsen¹, Jeffrey A. Engelman^{2,5}, and Kwok-Kin Wong^{3,4,5}

Abstract

ErbB3 is a critical activator of phosphoinositide 3-kinase (PI3K) signaling in epidermal growth factor receptor (EGFR; ErbB1), ErbB2 [human epidermal growth factor receptor 2 (HER2)], and [hepatocyte growth factor receptor (MET)] addicted cancers, and reactivation of ErbB3 is a prominent method for cancers to become resistant to ErbB inhibitors. In this study, we evaluated the *in vivo* efficacy of a therapeutic anti-ErbB3 antibody, MM-121. We found that MM-121 effectively blocked ligand-dependent activation of ErbB3 induced by either EGFR, HER2, or MET. Assessment of several cancer cell lines revealed that MM-121 reduced basal ErbB3 phosphorylation most effectively in cancers possessing ligand-dependent activation of ErbB3. In those cancers, MM-121 treatment led to decreased ErbB3 phosphorylation and, in some instances, decreased ErbB3 expression. The efficacy of single-agent MM-121 was also examined in xenograft models. A machine learning algorithm found that MM-121 was most effective against xenografts with evidence of ligand-dependent activation of ErbB3. We subsequently investigated whether MM-121 treatment could abrogate resistance to anti-EGFR therapies by preventing reactivation of ErbB3. We observed that an *EGFR* mutant lung cancer cell line (HCC827), made resistant to gefitinib by exogenous heregulin, was resensitized by MM-121. In addition, we found that a *de novo* lung cancer mouse model induced by *EGFR* T790M-L858R rapidly became resistant to cetuximab. Resistance was associated with an increase in heregulin expression and ErbB3 activation. However, concomitant cetuximab treatment with MM-121 blocked reactivation of ErbB3 and resulted in a sustained and durable response. Thus, these results suggest that targeting ErbB3 with MM-121 can be an effective therapeutic strategy for cancers with ligand-dependent activation of ErbB3. *Cancer Res*; 70(6); 2485–94. ©2010 AACR.

Introduction

The ErbB family of receptor tyrosine kinases includes epidermal growth factor (EGF) receptor (EGFR), ErbB2 (HER2), ErbB3 (HER3), and ErbB4 (HER4). Over the past 10 years, it has become evident that many epithelial cancers require EGFR or HER2 signaling for their growth and survival. Agents targeting EGFR have become widely used for the treatment of lung, colon, and head and neck cancers, whereas agents

targeting HER2 are commonly used to treat *HER2* amplified breast cancers. Inhibitors of EGFR and HER2 come in the form of small molecule tyrosine kinase inhibitors (TKI) and targeted antibodies.

Several recent studies have found that those cancers that are sensitive to EGFR or HER2 inhibitors are unique in that phosphoinositide 3-kinase (PI3K) signaling is under the sole control of either EGFR or HER2, respectively. For these inhibitors to be effective, they must lead to downregulation of the PI3K/AKT pathway (1–4). Prior studies have identified ErbB3, a kinase dead member of the ErbB family, as the key activator of PI3K/AKT signaling in EGFR addicted cancers (2, 5). In these cells, ErbB3 is tyrosine phosphorylated in an EGFR-dependent manner and then directly binds PI3K. Upon inhibition of EGFR, ErbB3 phosphorylation is abrogated, it no longer binds PI3K, and there is loss of PI3K/AKT signaling (2, 5). Furthermore downregulation of ErbB3 using short hairpin RNA leads to a decrease in AKT phosphorylation in EGFR addicted cancers (2). Similarly, ErbB3 is the major activator of PI3K in *HER2* amplified breast cancers (reviewed in ref. 6), and trastuzumab treatment leads to loss of ErbB3 phosphorylation, dissociation between ErbB3 and PI3K, and loss of AKT phosphorylation in these cancers (4). Thus, signaling through ErbB3 is the major mechanism of PI3K/AKT activation in both EGFR- and HER2-driven cancers.

Authors' Affiliations: ¹Merrimack Pharmaceuticals, Inc., Cambridge, Massachusetts; ²Massachusetts General Hospital Cancer Center, Charlestown, Massachusetts; ³Department of Medical Oncology, Dana-Farber Cancer Institute; ⁴Ludwig Center at Dana-Farber/Harvard Cancer Center; ⁵Department of Medicine, Harvard Medical School, Boston, Massachusetts; and ⁶Cell Signaling Technology, Danvers, Massachusetts

Note: Supplementary data for this article are available at Cancer Research Online (<http://cancerres.aacrjournals.org/>).

B. Schoeberl, A.C. Faber, and D. Li contributed equally to this work.

Corresponding Author: Jeffrey A. Engelman, Massachusetts General Hospital, Charlestown, MA 02129. Phone: 617-724-7298; Fax: 617-724-9648; E-mail: jengelma@partners.org or Kwok-Kin Wong, Dana-Farber Cancer Institute, Boston, MA 02115. Phone: 617-632-6084; Fax: 617-582-7839; E-mail: kwong1@partners.org.

doi: 10.1158/0008-5472.CAN-09-3145

©2010 American Association for Cancer Research.

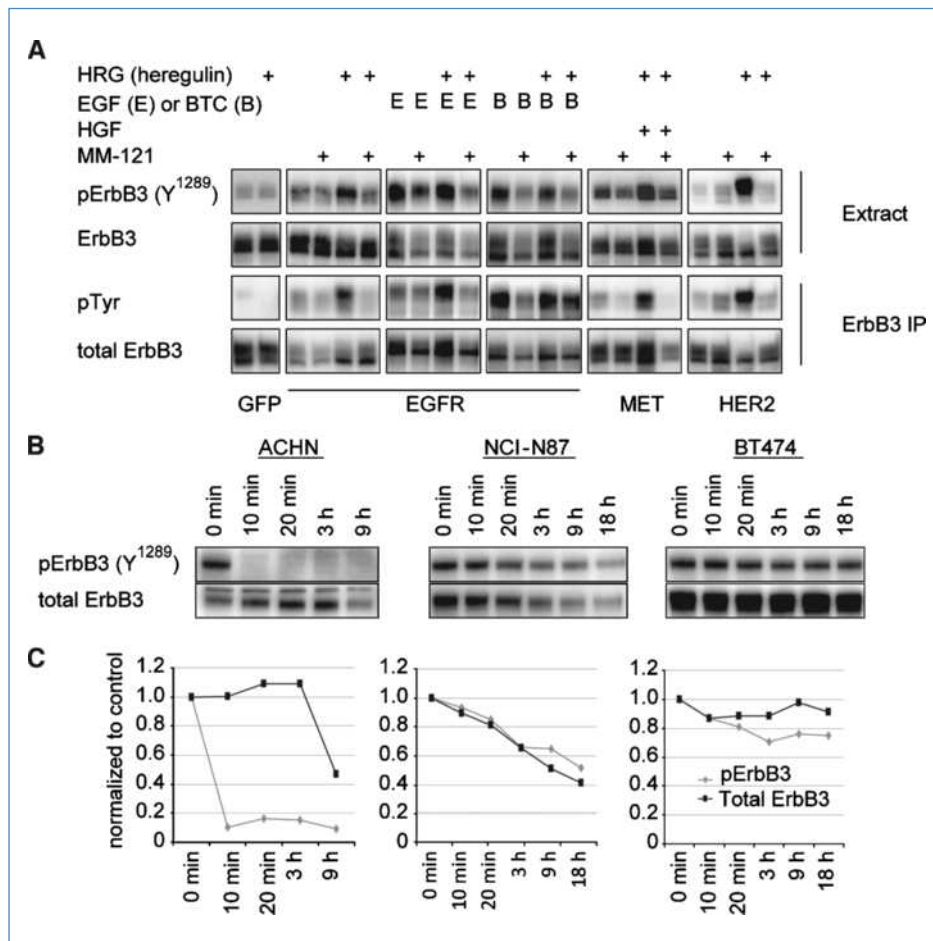


Figure 1. MM-121 inhibits ligand-induced ErbB3 phosphorylation by blocking ligand activation and by receptor downregulation. **A**, CHO cells were transiently transfected with vectors expressing ErbB3 (FLAG tagged) and either GFP (control), EGFR, MET, or HER2. The transfected cells were treated with $\pm 170 \mu\text{g/mL}$ MM-121 overnight and then treated with the indicated ligands for 10 min before lysis. The cell lysates were probed with the indicated antibodies (top two panels) and were immunoprecipitated with an anti-FLAG antibody and probed with an anti-phosphorylated tyrosine antibody. **B**, three representative cell lines, ACHN (renal), NCI-N87 (gastric), and BT-474 (mammary), were treated with MM-121 for the indicated times and immunoblotted for total ErbB3 and phosphorylated ErbB3 expression levels. **C**, densitometric analysis was performed on the Western blots presented in **B**.

Although EGFR- and HER2-driven cancers often respond to anti-ErbB therapies, these cancers invariably become resistant. We and others have learned that some cancers become resistant when they reactivate ErbB3 signaling. There are examples of resistance that implicate EGFR, HER2, and MET in reactivating ErbB3 (5, 7–9). In addition, heregulin-induced activation of HER2-ErbB3 heterodimers has also been associated with resistance to EGFR inhibitors (10). Because ErbB3 is a focal point for both the initial effectiveness of EGFR and HER2 therapies as well as the development of drug resistance, there is considerable effort to develop methods to directly target ErbB3 with therapeutics. Unlike other ErbB family members, ErbB3 is characterized by the lack of kinase activity (11). Thus, antibodies directed against ErbB3 may be the most effective method to disrupt its function. In this study, we provide the first evaluation of this class of therapeutics by examining the efficacy of the anti-ErbB3 antibody MM-121, which is currently in clinical development.

Materials and Methods

Cell lines and reagents. Cell lines used in this study were obtained from the National Cancer Institute's

Developmental Therapeutics Program,⁷ wherein these cell lines have been maintained in cryopreservation and in culture, and they have been subjected to strict quality controls, including adventitious agent testing, human isoenzyme analysis, karyology, morphologic and immunocytochemical characterization, and DNA fingerprinting. The cell lines were kept below 10 passages or passaged for <6 mo after receipt or resuscitation in our laboratories. All cell lines were maintained in RPMI 1640 supplemented with 10% FCS, 2 $\mu\text{mol/L}$ L-glutamine, and Pen-Strep and grown in a humidified atmosphere of 5% CO₂, 95% air at 37°C, unless otherwise indicated. Chinese hamster ovary (CHO) cells were described previously (2).

Western blot analyses of total ErbB3 and phosphorylated ErbB3 in cancer cell lines. ACHN, NCI-N87, and BT-474 cells were treated with 170 $\mu\text{g/mL}$ of MM-121. Cells were lysed, blotted, and analyzed for total and phosphorylated ErbB3 at 0 min, 10 min, 30 min, 3 h, 9 h, and 18 h. Proteins from Western blots were quantified using Syngene GeneTools software program. Phosphorylated ErbB3/ErbB3 ratios of MM-121-treated lysates were normalized to the corresponding control (same

⁷ <http://www.dtp.nci.nih.gov>

treatment, without MM-121). Please see supplementary data for additional experimental details.

MM-121 and cetuximab treatment in EGFR T790M-L858R mice. Mouse lung cancer model driven by doxycycline-inducible EGFR T790M-L858R expression was reported previously (12). Mice were put on doxycycline diet (Research Diets, Inc.) at the age of 6 wk and imaged by magnetic resonance imaging (MRI) to document tumor burden after another 6 to 8 wk. The mice were then randomly divided into placebo, MM-121, cetuximab (BMS Pharmaceuticals), and MM-121 plus cetuximab treatment groups. MM-121 and cetuximab groups were all given a 1 mg/mouse drug dose through i.p. injection every 3 d. Each antibody was given at different days in combination treatment group. Mice were imaged by MRI at 2 and 4 wk following initiation of treatment and then sacrificed for histologic analysis. The protocol for the animal work was approved by Dana-Farber Cancer Institute Institutional Animal Care and Use Committee, and the mice were housed in a pathogen-free environment at Harvard School of Public Health. Please see supplementary materials for further experimental details.

Determination of hyperplanes. We attempted to characterize the differences between MM-121 xenograft responders and nonresponders based on the measurements of ErbB1-3, β -cellulin (BTC) secretion, and heregulin (HRG1- β 1) expression in three untreated tumors reported as means and SD in Supplementary Table S1. To be able to take the \log_{10} of the zero entries in Supplementary Table S1, we replaced zero with a very small number by using the smallest nonzero value of the data and dividing it by 10. The support vector machine (SVM) algorithm (13, 14) was used to define a boundary that distinguished the xenograft responders and nonresponders based on these five measurements. We used a Matlab (Mathworks) toolbox that can be downloaded from the ISIS Web site.⁸ Briefly, our implementation of the algorithm computes a linear, multidimensional boundary or hyperplane that separates the two classes such that the distance (or "margin") between them is maximized.

Results

MM-121 blocks ligand-dependent activation of ErbB3.

Using a systems biology approach, we previously identified ErbB3 to be a key node in the ErbB signaling network (15). The fully human anti-ErbB3 monoclonal antibody MM-121 was identified from a phage display library screen based on computationally driven selection criteria (15). MM-121 binds with high affinity to ErbB3 and blocks the binding of its ligand, heregulin, to ErbB3 and inhibits BTC-induced phosphorylation of ErbB3. ErbB3 is known to form heterodimers with a variety of receptors within the ErbB family like EGFR (16) and ErbB2/Her2, and it also associates with MET (5, 17). To assess if MM-121 could inhibit ligand-induced activation of ErbB3 by different receptors, ErbB3 was cotransfected with green fluorescent protein (GFP; control), EGFR, MET, or

ErbB2/HER2 in CHO cells. The transfected cells were then treated with the indicated ligands in the absence or presence of MM-121 as shown in Fig. 1A. ErbB3 phosphorylation was measured using an antibody that specifically recognizes ErbB3 that is phosphorylated on tyrosine Y¹²⁸⁹. In addition, to more globally assess ErbB3 tyrosine phosphorylation, total ErbB3 was immunoprecipitated from the cells and probed with an anti-phosphorylated tyrosine antibody. MM-121 effectively blocked ligand-induced phosphorylation of ErbB3 by all of the coreceptors as evidenced by reduction at the Y¹²⁸⁹ site and total ErbB3 phosphorylated tyrosine levels (Fig. 1A). However, the effect on total ErbB3 levels following the different cotransfections was more variable (please see quantification of phosphorylated ErbB3/total ErbB3 ratios in Supplementary Fig. S1). Of note, MM-121 decreased ErbB3 expression in CHO cells transfected with EGFR in the presence and absence of the ligands EGF or BTC (Fig. 1A) but not with HER2 or MET. In CHO cells cotransfected with MET and ErbB3, stimulation with heregulin and hepatocyte growth factor resulted in a potent phosphorylation of ErbB3 that was inhibited by MM-121. In CHO cells cotransfected with HER2 and ErbB3, MM-121 potentially blocked heregulin-induced phosphorylation of ErbB3. Of note, even when ErbB3 internalization in MALME 3M cells was disrupted with cold temperature or a transglutaminase inhibitor, MM-121 inhibited ErbB3 phosphorylation similarly (Supplementary Fig. S2). Thus, these studies suggest that MM-121 can potentially inhibit ligand-induced activation of ErbB3. However, MM-121 may be less effective when ErbB3 phosphorylation does not require ligand.

To further address the effects of MM-121 on both ErbB3 phosphorylation and expression, we treated three cancer cell lines, ACHN, NCI-N87, and BT-474, with MM-121 (Fig. 1B and C). As will be described below, these cell lines are respectively sensitive, moderately sensitive, and resistant to MM-121 *in vivo*. Interestingly, we observed that MM-121 effects ErbB3 through at least two potential mechanisms. In ACHN cells, there was clear loss of ErbB3 phosphorylation before any effect on ErbB3 protein expression, presumably due to inhibition of ligand binding. Contrastingly, in the NCI-N87 cells, the trajectory of ErbB phosphorylation mirrored that of ErbB3 expression. This result implies that receptor downregulation in NCI-N87 cells may contribute to the loss of ErbB3 phosphorylation. Lastly, in BT-474 cells, MM-121 had a minimal effect on either ErbB3 phosphorylation or protein expression levels. Of note, these cells have marked HER2 amplification and ligand-independent activation of ErbB3 (Supplementary Table S1).

In addition, fluorescence-activated cell sorting and Western blot analyses determined that the effect of MM-121 on ErbB3 expression varied across other cell lines as well. For example, MM-121 effectively downregulated expression of ErbB3 in MALME 3M cells, but not in DU145 cells (Supplementary Fig. S3).

MM-121 shows efficacy *in vivo* against a subset of cancer cell lines. To understand the effect of MM-121 on downstream signaling, we studied the ability of MM-121 to inhibit signaling *in vitro* in ACHN (renal), Du145 (prostate), OvCAR8 (ovarian), and ADRr (ovarian) cells in the presence

⁸ <http://www.isis.ecs.soton.ac.uk/resources/svminfo/>

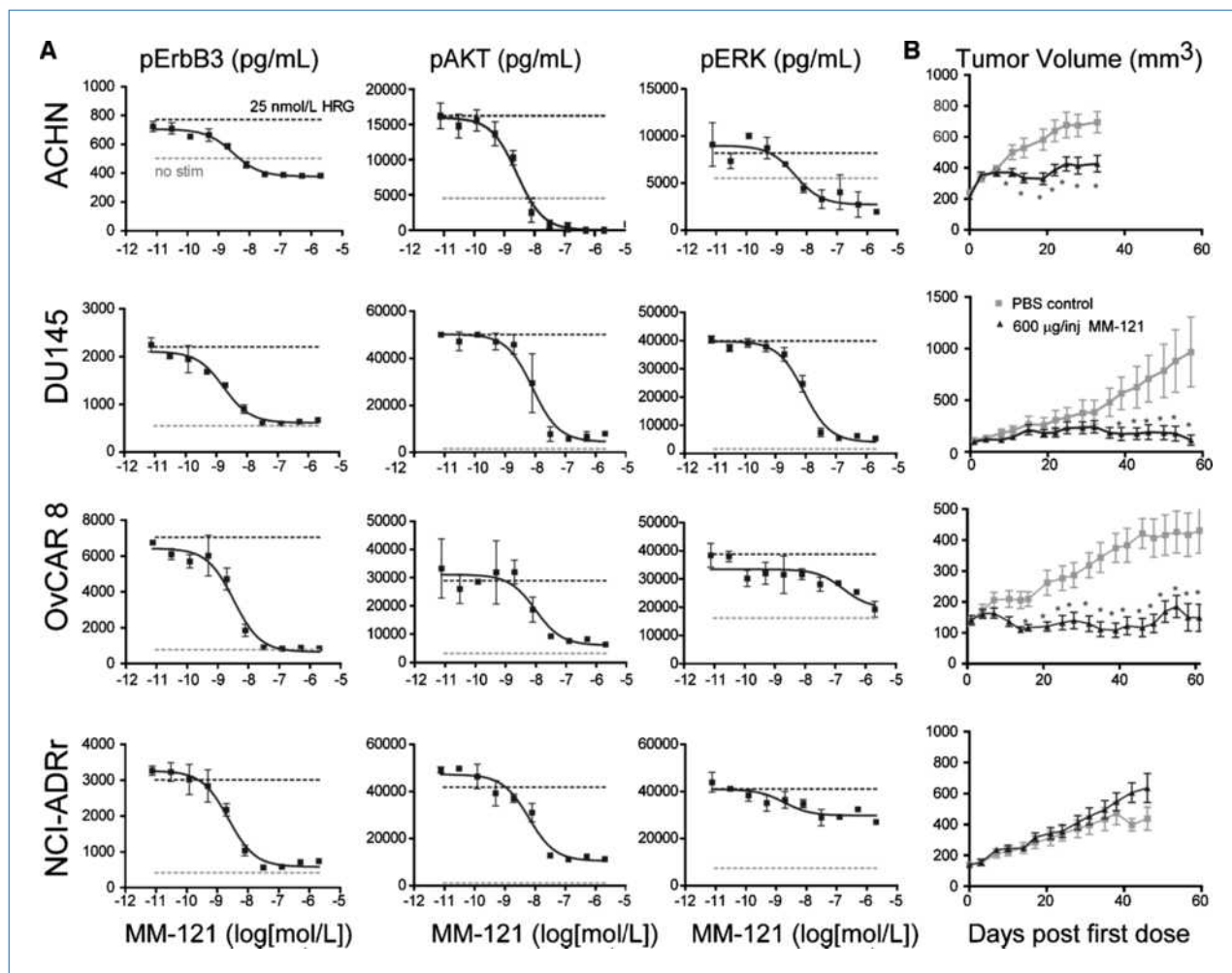


Figure 2. MM-121 blocks ligand-induced activation of ErbB3 and shows activity *in vivo*. A, cells were cultured in 96-well plates and synchronized by 20 to 24 h serum starvation. The cells were then treated with MM-121 for 30 min and subsequently stimulated with 25 nmol/L heregulin (HRG1- β) for 10 min, washed once with cold PBS prior, and lysed. ELISA analysis of the cell lysates showed that MM-121 inhibited heregulin-induced ErbB3, AKT, and ERK phosphorylation (solid squares) compared with the 25 nmol/L heregulin control without MM-121 (black dotted line). Inhibitor IC₅₀ values were calculated by least squares fitting the dose-response data with a sigmoidal curve (solid black line). In most cases, maximal inhibition of pErbB3, pAKT, and pERK with MM-121 occurred near or below basal signaling levels as measured by the unstimulated control cells (gray dotted line). Points, mean of two separate experiments; bars, SD. B, efficacy of MM-121 on human cancer cell lines *in vivo*. ACHN, DU145, OVCAR8, and NCI-ADRr were injected s.c. as a Matrigel suspension into nude mice and allowed to grow to at least 150 mm³. Groups of 10 animals were each treated with vehicle control (PBS) or MM-121 every 3 d. SEM is shown for each point on the graph. Statistics were performed by Student's *t* test and significance relative to control is noted in the graph (*, *P* < 0.05).

of heregulin and BTC (Fig. 2A; Supplementary Fig. S4). We observed that MM-121 blocked the capacity of heregulin to stimulate ErbB3 and downstream AKT and extracellular signal-regulated kinase (ERK) phosphorylations in all cell lines. In cell lines that MM-121 reduced signal to levels equal to or below the unstimulated cells (Fig. 2A), MM-121 showed efficacy in subsequent *in vivo* studies (Fig. 2B). In the NCI-ADRr cell line wherein only partial inhibition of AKT and ERK phosphorylation in response to MM-121 was observed *in vitro*, MM-121 did not show efficacy *in vivo* (Fig. 2B). These findings were confirmed in independent experiments assessing the ability of MM-121 to inhibit basal ErbB3 phosphorylation (Supplementary Fig. S5). Similar experiments with BTC as the activating ligand were conducted; however, the

signal strength induced by BTC is often weaker compared with heregulin (Supplementary Fig. S3).

To more comprehensively evaluate the antitumor activity of MM-121 as a single-agent *in vivo*, we screened a panel of xenograft tumor models (Fig. 2B; Supplementary Fig. S6). Of the nine tumor models studied, we observed substantial tumor growth arrest in three tumor models (DU145, OVCAR8, and ACHN), modest tumor growth delay in two tumor models (NCI-87 and SKOV3), and no significant antitumor activity in the other four tumor models (NCI-ADRr, BT-474, IGROV1, and MALME 3M). If MM-121 treatment led to tumor stasis, the cell line was considered a "responder," and if there was no effect on tumor growth, the cell line was considered a "nonresponder." Importantly, we observed that

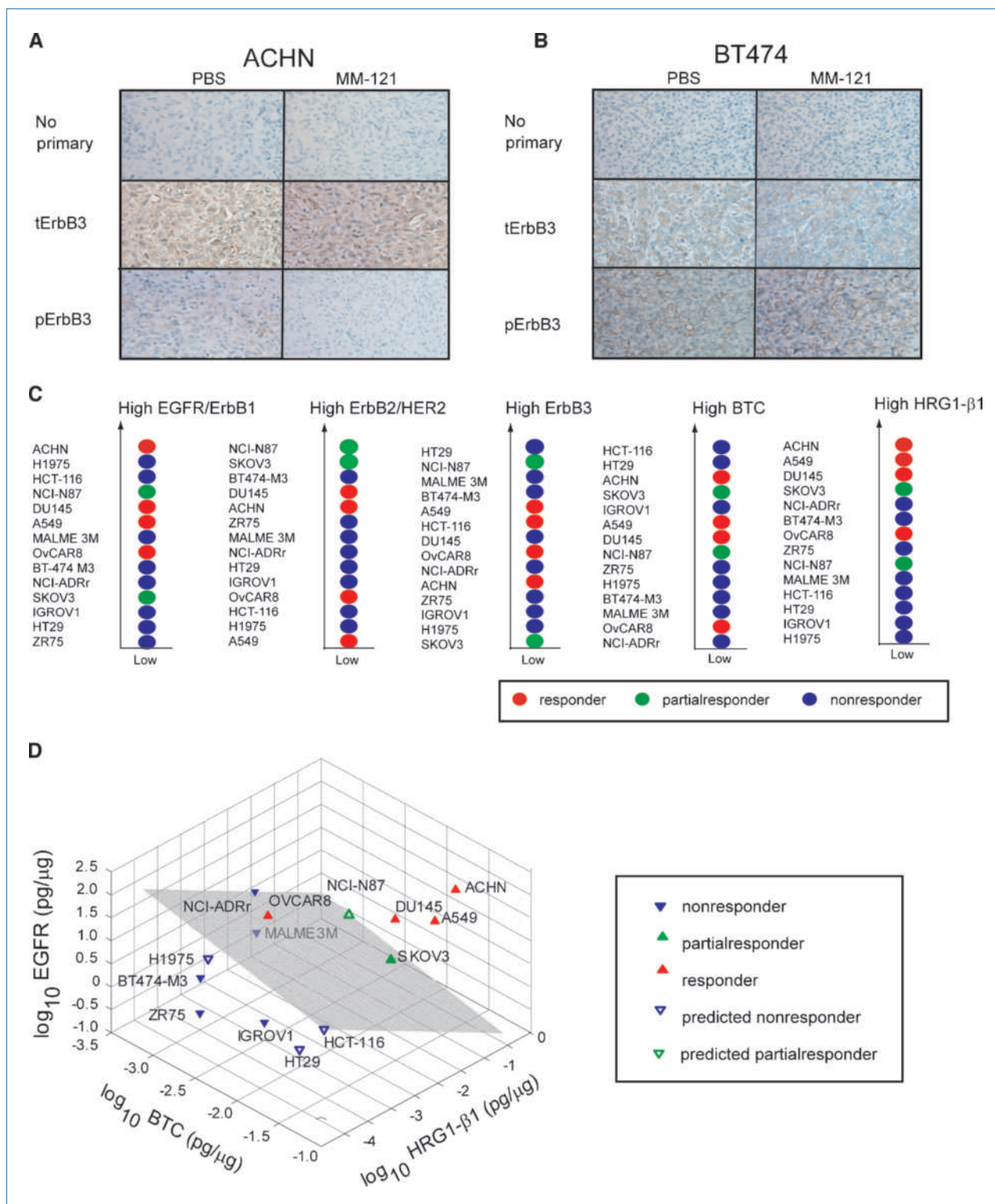


Figure 3. MM-121 shows *in vivo* efficacy in tumors with evidence of ligand-dependent activation of ErbB3. A and B, immunohistochemistry of ErbB3 and pErbB3 in ACHN (responder) and BT-474 (nonresponder) tumors at the end of the efficacy studies are shown in Supplementary Fig. S6. Magnification, 20 \times . C, MM-121 responsive and nonresponsive xenografts were classified based on a single feature of ErbB receptor and ligand (BTC and heregulin) expression values. MM-121 responders (red) and partial responders (green) had higher levels of ErbB1, BTC, and heregulin (HRG1-β1) than nonresponders (blue). Receptor and ligand values are listed in Supplementary Table S1. D, separating planes (gray) were determined with the SVM algorithm using HRG1-β1 and BTC as predictor variables.

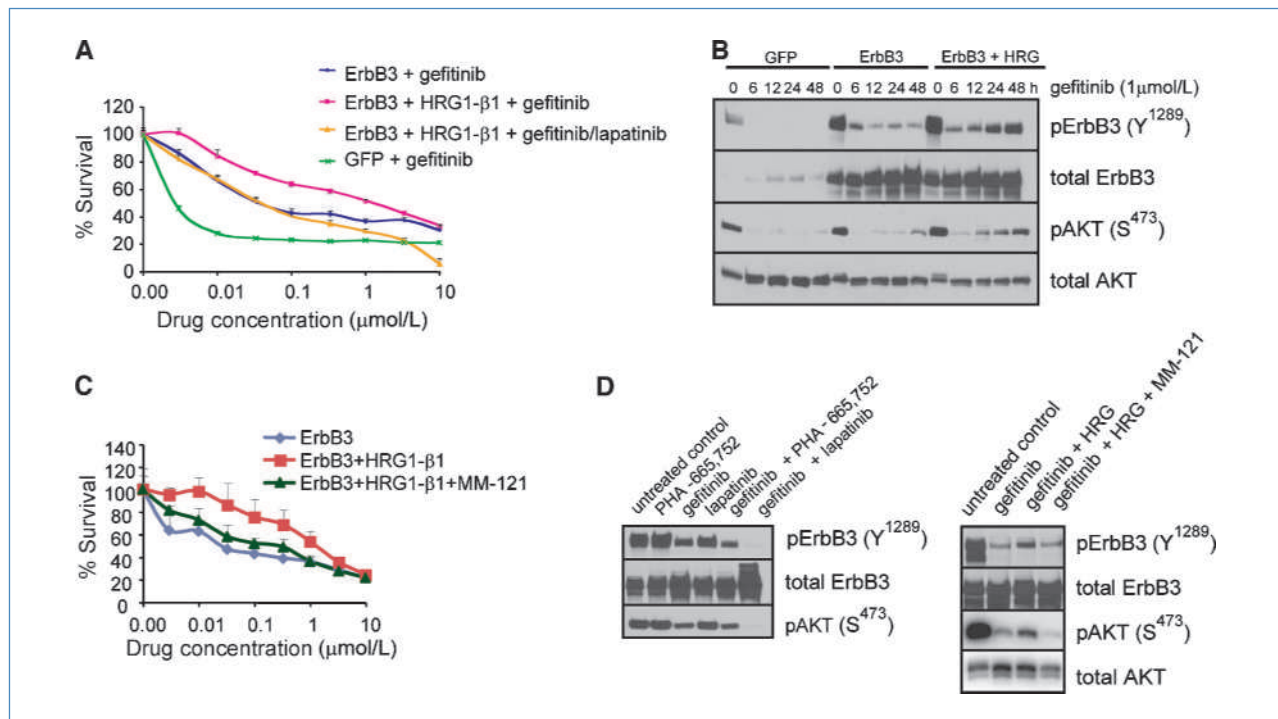


Figure 4. MM-121 overcomes heregulin-induced resistance to anti-EGFR therapies. A, HCC827 cells were engineered to overexpress GFP (control) or ErbB3 using retrovirally encoded ErbB3 as described previously (2). GFP and ErbB3-overexpressing HCC827 cells were treated with increasing concentrations of gefitinib, and cell survival was determined using a syto60 assay. Survival assays were done in the presence of heregulin (50 ng/mL) where indicated. Lapatinib was used in addition to gefitinib where indicated. Lapatinib shifts the survival curve to negate the effect of heregulin. B, Western blots of the parental and ErbB3-overexpressing cells in the presence or absence of heregulin. C, ErbB3-overexpressing HCC827 cells were treated with \pm heregulin in the presence or absence of MM-121 (170 μ g/mL) for a 72-h cell survival syto60 assay. D, Western blots of ErbB3-overexpressing HCC827 cells treated with heregulin in the presence of either the MET inhibitor, PHA-665,752 (1 μ mol/L), gefitinib (1 μ mol/L), or lapatinib (1 μ mol/L) or in the indicated combinations for 6 h (left). The same cells were treated with gefitinib (1 μ mol/L) \pm heregulin (50 ng/mL) \pm MM-121 (170 μ g/mL) for 6 h (right). The lysates were probed with the indicated antibodies.

short-term exposure to MM-121 blocked ErbB3 phosphorylation, induced apoptosis, and reduced proliferation in one of the responding tumor models (Supplementary Fig. S7). Upon investigating the expression of phosphorylated ErbB3 and ErbB3 at the end of the treatment study, we observed that MM-121 continued to inhibit phosphorylated ErbB3 in the responding ACHN cells, but ErbB3 total protein expression remained intact (Fig. 3A). However, MM-121 had no effect on phosphorylated ErbB3 or total ErbB3 in the nonresponder BT474 cells (Fig. 3B). These results mirror those obtained from the *in vitro* studies (Fig. 1B).

Assessment of ErbB biomarkers to predict response to MM-121 *in vivo*. To gain a better understanding of the responding versus nonresponding cell lines *in vivo*, we quantified receptor expression levels in the untreated tumors established from the cell lines of interest (Supplementary Table S1). Because BTC and heregulin were both potent ligands for activating ErbB3 phosphorylation, these two ligands were assessed as well (15). ErbB4 expression levels were essentially undetectable and were thus omitted in the subsequent analysis. From all the ligands and receptors quantified in the different tumor types, the heregulin expression levels seem to be the best single feature separating responding from nonresponding cell lines (Fig. 3C), but no

clear separation was obtained by assessment of a single feature.

To distinguish responders and nonresponders using two or more variables, we used a computational model by using a SVM algorithm (13, 14). The SVM uses the given set of training xenograft studies that are each characterized by a set of features (ligand and receptor expression levels shown in Supplementary Table S1) to distinguish responders and nonresponders. An SVM model maps the xenograft responses as points in the feature space, so that the responders and nonresponders are divided by a clear gap, represented by a hyperplane. The SVM constructs a separating hyperplane in the feature space, which maximizes the margin between the two data sets (responder versus nonresponder). New xenograft studies are then mapped into that same space and predicted to belong to a category based on which side of the gap they fall on. Because parsimonious models are more robust to noisy training data (18), we applied the SVM algorithm with all possible combinations of input variables and then ranked the hyperplanes based on their margin and number of dependent variables. The hyperplane that separated the two classes with the largest margin and the fewest variables consisted of ErbB1, BTC, and HRG1- β 1 (shown in Fig. 3D). Our rationale to use the protein expression level of HRG1- β 1 and BTC as the

two ligands to characterize the xenograft tumors in this modeling algorithm is based on our previous findings that, from a panel of nine different ErbB ligands, HRG1-b1 and BTC are the two most potent inducers of ErbB3 phosphorylation (15).

Despite the relatively small number of xenograft studies used as a training set, the SVM model was able to accurately predict that the HCT116, HT29, and H1975 cells would be non-responders and the NCI-N87 cells would be partial responders (Fig. 3D; Supplementary Fig. S6). We note that algorithms, such as SVM, only identify trends in the data and generate hypotheses requiring continued interrogation as this antibody enters the clinic. In addition, we found that *HER2* amplification is seemingly associated with resistance to MM-121

(Supplementary Table S1), likely because these cancers probably are driven by ligand-independent activation of ErbB3 (see BT474 in Supplementary Fig. S6 and Supplementary Table S1). Based on the earlier data (Supplementary Fig. S5), this would suggest that cancers in which HER2 is driving ErbB3 phosphorylation in a ligand-dependent manner may be the ones that are most sensitive to MM-121 as a single agent.

Interestingly, MM-121-sensitive ACHN cells expressed ~500 times more heregulin and ~100 times more BTC than the MM-121-resistant MALME 3M cells (Fig. 3C), whereas both cell lines showed similar expression level of HER2 receptors. It thus seems that the ligand expression level is a key indicator of response to MM-121. Indeed, all of the

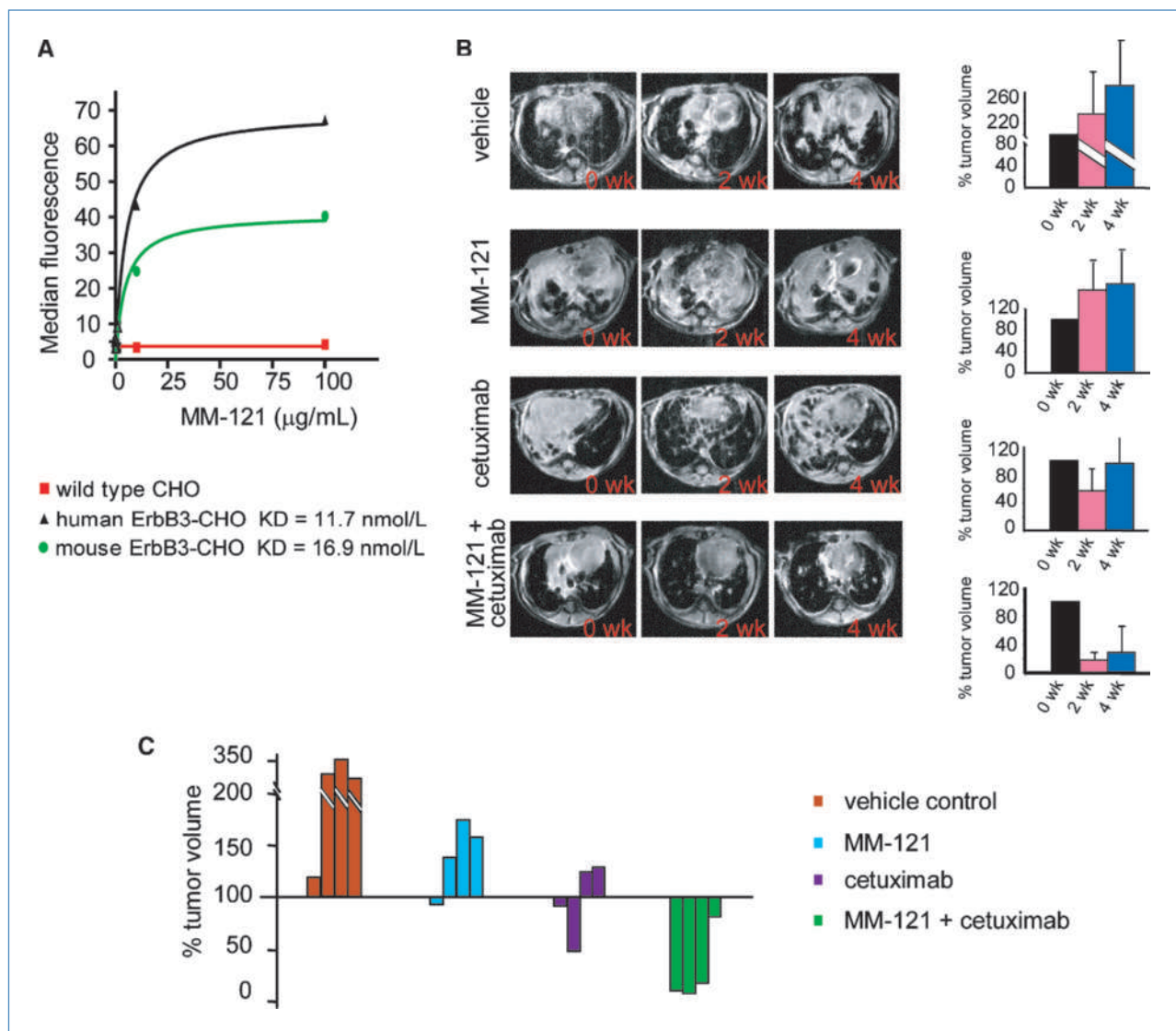


Figure 5. MM-121 and cetuximab combination induces durable tumor regression in mouse lung cancer model driven by doxycycline-inducible EGFR T790M-L858R. A, CHO cells transfected with mouse or human ErbB3 bind MM-121 with a similar affinity. B, each EGFR T790M-L858R mouse with lung cancer was treated either with placebo, 1 mg of MM-121, 1 mg of cetuximab, or combination of both antibodies through i.p. injection every 3 d. MRI images of a representative mouse from indicated groups at 2 and 4 wk of treatment were shown in each row, to the right of corresponding MRI images. Relative tumor regression of all of the four mice in each group is shown in the bar graph on the right (initial tumor volume of each mouse was normalized to 100%). C, relative tumor regression rate of each individual mouse at 4 wk of indicated treatments is shown.

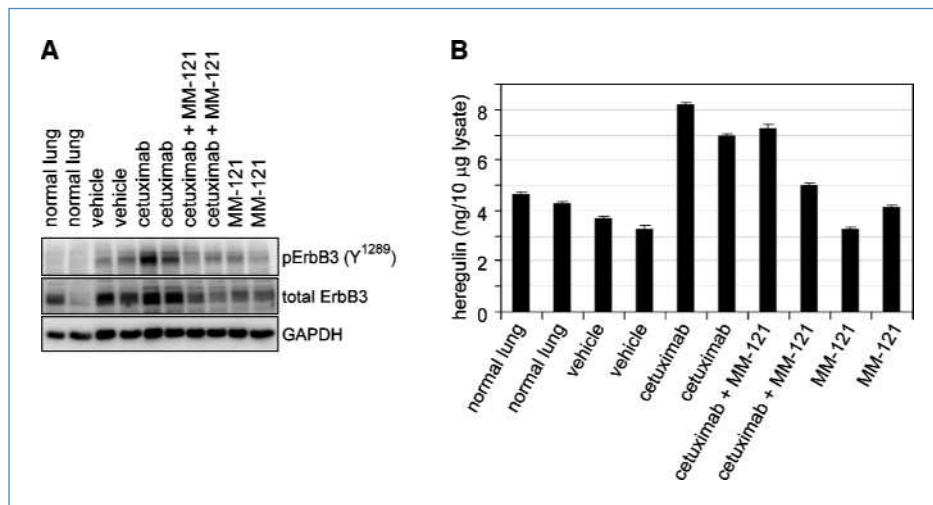


Figure 6. MM-121 blocks reactivation of ErbB3 upon development of resistance to cetuximab. Mice were treated as indicated in Fig. 5. At the end of the 4-wk treatment, the mouse lungs were harvested and protein lysates were probed with the indicated antibodies (A) and subjected to an ELISA (B) to determine heregulin levels.

responding cell lines expressed high levels of either heregulin or BTC, confirming our earlier observation that MM-121 is likely active in cancers with ligand-dependent ErbB3 signaling.

MM-121 can overcome heregulin-induced resistance to EGFR inhibitors. Over the past few years, the critical role of ErbB3 in EGFR-, HER2-, and MET-driven cancers has become clear. Indeed, recent evidence suggests that cancers can acquire resistance to EGFR and HER2 by adopting a novel way to activate ErbB3 (2, 5, 8, 9). Our studies show that MM-121 can potently block ligand-induced activation of ErbB3. Thus, we hypothesized that this antibody could overcome ligand-dependent, acquired resistance to EGFR inhibitors, a mechanism shown to cause gefitinib resistance (10). Accordingly, heregulin promoted gefitinib resistance in HCC827 cells (*EGFR* exon 19 deletion mutation and *EGFR* amplified) overexpressing ErbB3 (Fig. 4A and C). The ErbB3-overexpressing cells stimulated with heregulin maintained ErbB3 and AKT phosphorylation in the presence of gefitinib (Fig. 4B). Indeed, HER2 seemed to promote heregulin-induced ErbB3 phosphorylation in the presence of gefitinib. Only the combination of gefitinib and lapatinib abolished ErbB3 and AKT phosphorylation (Fig. 4D, left). Similar to lapatinib, MM-121 reversed the resistance promoted by heregulin (Fig. 4C). Accordingly, MM-121 blocked heregulin-induced rescue of ErbB3 and AKT phosphorylation in the presence of gefitinib (Fig. 4D, right).

We next assessed the activity of MM-121 in a genetically engineered mouse model of *in situ* lung cancers that are induced by a doxycycline-inducible human *EGFR T790M-L858R* transgene that is expressed specifically in the lung epithelium (12). This genetically engineered mouse model mimics patients with acquired resistance to EGFR TKIs that is caused by acquisition of the secondary T790M mutation (19). These mice develop aggressive lung adenocarcinomas upon continuous administration of doxycycline in their diets. Similar to patients with the T790M resistance mutation, these cancers are resistant to erlotinib (20). We were able to use MM-121 for these experiments because MM-121 cross-reacts potently with mouse ErbB3 (Fig. 5A; Supplementary Fig. S8).

When we treated mice harboring established tumors with the EGFR antibody cetuximab, there was a modest response at 2 weeks, but this response was transient, with clear resistance at 4 weeks (Fig. 5B and C). Interestingly, this resistance was associated with increased phosphorylated ErbB3 in the *EGFR T790M-L858R* tumors compared with untreated controls (Fig. 6A). The observed increase in phosphorylated ErbB3 levels in the presence of cetuximab correlates with the observed increased levels of heregulin (Fig. 6B). Addition of MM-121 to cetuximab downregulated ErbB3, and the increase in ErbB3 phosphorylation was observed following single-agent cetuximab therapy. Importantly, the combination of MM-121 and cetuximab led to a more dramatic and sustained response (Fig. 5B).

Discussion

In this study, we have evaluated the *in vitro* and *in vivo* efficacy of a new type of targeted therapy, an anti-ErbB3 antibody, MM-121. ErbB3 has emerged as a critical partner in EGFR, HER2, and MET oncogene addicted cancers. In particular, its many tyrosine phosphorylation sites serve as potent modules to activate intracellular signaling, especially the PI3K pathway (21, 22). In many EGFR- and HER2-driven cancers, ErbB3 tyrosine phosphorylation is necessary for transmittal of these downstream signaling events, and treatment with the appropriate TKI leads to loss of ErbB3 phosphorylation and cessation of downstream signaling. Recent studies have revealed that reactivation of ErbB3/PI3K signaling is a major mechanism of acquired resistance to EGFR and HER2 inhibitors (5, 8, 9, 23). In particular heregulin-induced activation of ErbB3 may cause resistance to gefitinib (10). For these reasons, there has been great enthusiasm for targeting ErbB3 directly as a therapy. However, unlike other ErbB family members, ErbB3 is kinase dead (11). Thus, it seems that antibody therapies directed against the extracellular domain of ErbB3 seem to be the most effective method to disrupt its function.

The *in vivo* activity of MM-121, an anti-ErbB3 antibody, was assessed in this study. This antibody was chosen for clinical

development because it potently blocks ligand-dependent activation of ErbB3 (Figs. 1 and 2; Supplementary Figs. S4 and S5). In this study, we also provide evidence that MM-121 blocks ligand binding and leads to receptor internalization and degradation. Interestingly, although the antibody blocks ligand-dependent activation of ErbB3 phosphorylation in all cell lines examined, antibody-mediated receptor internalization and downregulation seems to be cell line dependent. Our results also imply that, in the presence of a strong autocrine ligand activation of ErbB3 as in the ACHN or DU145 cells, MM-121 blocks ligand activation of ErbB3 without downregulating ErbB3 expression (Figs. 1B and 3A). Yet, in other cell lines, such as the NCI-N87 cells, receptor internalization and degradation may contribute to MM-121 activity (Fig. 1B). However, we currently do not know why MM-121 downregulates ErbB3 expression in some cells, but not others. Of note, for MM-121 to be effective in a ligand-independent manner (i.e., only by downregulation of ErbB3), treatment would need to result in the elimination of most of the ErbB3 protein. It would seem that in cancers with ligand-independent activation of ErbB3 (e.g., *HER2*-amplified cancers) MM-121 does not sufficiently downregulate ErbB3 to low enough levels and thus has minimal effect on cell viability.

MM-121 exerted substantial antitumor activity in three xenograft tumor cell lines (DU145, OVCAR8, and ACHN) as a single-agent therapy. However, it was ineffective in many other cancer models. Of particular note, this antibody did not block ErbB3 phosphorylation and was ineffective in the *HER2*-amplified cancer cell lines (Supplementary Table S1; Supplementary Figs. S5 and S6). We hypothesize that the high concentration of *HER2* receptors on the membrane likely obviates the need for ligand-dependent activation of ErbB3. On the other hand, it is not surprising that cancers with high ligand expression in non-*HER2*-amplified cancers were the most responsive to single-agent therapy (Fig. 3). Although these biomarkers are useful toward understanding the biology behind responsiveness to this antibody, it is hard to predict how applicable they will be in the clinical development of this antibody, and more work needs to be done to elucidate possible biomarker-response relationships. Indeed, predicting response may require a panel of biomarkers that will likely include heregulin. Based on these findings, we hypothesize that MM-121 will be most effective when treating ligand-dependent tumors. Of note, because ovarian cancers, pancreatic cancers, papillary thyroid cancers, and medulloblastomas express heregulin in >70% of analyzed primary tumors (24), therapy using MM-121 may show activity in these malignancies.

There are likely some cancers that express phosphorylated ErbB3, yet ErbB3 is not critical for the growth and survival. In these cancers, MM-121 may downregulate ErbB3 phosphory-

lation and/or total ErbB3 without therapeutic effect as a single agent. In such cancers, PI3K-AKT signaling may not be solely dependent on ErbB3 and/or downregulation of PI3K-AKT may not be sufficient to induce growth arrest and/or apoptosis. In these cancers, there may be a benefit for combining MM-121 with other targeted therapies.

Recent studies have highlighted the central role of reactivation of ErbB3 signaling as a mechanism of acquired resistance to EGFR- and HER2-based therapies. Therefore, an effective ErbB3 antibody may retard the development of resistance to these inhibitors. In this study, we observed that MM-121 potently prevented resistance to anti-EGFR-based therapies *in vitro* and *in vivo* (Figs. 4–6). Importantly, we assessed the activity of MM-121 in the genetically engineered mouse model of lung cancers driven by *EGFR T790M-L858R*. The “gatekeeper” T790M mutation in *EGFR* is observed in 50% of lung cancers that become resistant to the EGFR TKIs, gefitinib, and erlotinib (19, 20). This mouse model faithfully recapitulates human lung cancers that harbor this mutation in that tumors derived from these mice are resistant to gefitinib yet sensitive to irreversible EGFR inhibitors (12, 25). These cancers showed a transient response to cetuximab (Fig. 5). However, resistance to cetuximab was associated with an activation of ErbB3 phosphorylation and increased expression of heregulin (Fig. 6). This suggests that activation of ErbB3 in a ligand-dependent manner caused resistance. Importantly, addition of MM-121 to cetuximab blocked the reactivation of ErbB3 and led to a greater and more durable response. Taken in its entirety, these data provide the clinical basis for the evaluation of MM-121 in combination with anti-EGFR- and HER2-based therapies. This may lead to more impressive responses and improved times to progression for patients with EGFR- or HER2-driven cancers.

Disclosure of Potential Conflicts of Interest

No potential conflicts of interest were disclosed.

Grant Support

Dana-Farber–Harvard Cancer Center Lung Cancer Specialized Program of Research Excellence (SPORE) grant P50 CA090578 (J.A. Engelman and K-K. Wong); NIH grants K08 AG024004 (K-K. Wong), R01 AG2400401 (K-K. Wong), R01 CA122794 (K-K. Wong), R01 CA140594 (J.A. Engelman and K-K. Wong), K08 grant CA120060 (J.A. Engelman), R01CA137008 (J.A. Engelman), and R01CA140594 (J.A. Engelman); DF/HCC Gastrointestinal Cancer SPORE P50 CA127003 (J.A. Engelman); American Association for Cancer Research (J.A. Engelman); V Foundation (J.A. Engelman); American Cancer Society RSG-06-102-01-CCE (J.A. Engelman); and Ellison Foundation Scholar (J.A. Engelman).

The costs of publication of this article were defrayed in part by the payment of page charges. This article must therefore be hereby marked *advertisement* in accordance with 18 U.S.C. Section 1734 solely to indicate this fact.

Received 08/22/2009; revised 01/08/2010; accepted 01/11/2010; published OnlineFirst 03/09/2010.

References

- Bianco R, Shin I, Ritter CA, et al. Loss of PTEN/MMAC1/TEP in EGF receptor-expressing tumor cells counteracts the antitumor action of EGFR tyrosine kinase inhibitors. *Oncogene* 2003;22:2812–22.
- Engelman JA, Janne PA, Mermel C, et al. ErbB-3 mediates phosphoinositide 3-kinase activity in gefitinib-sensitive non-small cell lung cancer cell lines. *Proc Natl Acad Sci U S A* 2005;102:3788–93.
- Moulder SL, Yakes FM, Muthuswamy SK, Bianco R, Simpson JF, Arteaga CL. Epidermal growth factor receptor (HER1) tyrosine kinase inhibitor ZD1839 (Iressa) inhibits HER2/neu (erbB2)-overexpressing

- breast cancer cells *in vitro* and *in vivo*. *Cancer Res* 2001;61:8887–95.
4. Yakes FM, Chinratanalab W, Ritter CA, King W, Seelig S, Arteaga CL. Herceptin-induced inhibition of phosphatidylinositol-3 kinase and Akt is required for antibody-mediated effects on p27, cyclin D1, and antitumor action. *Cancer Res* 2002;62:4132–41.
 5. Engelman JA, Zejnullahu K, Mitsudomi T, et al. MET amplification leads to gefitinib resistance in lung cancer by activating ERBB3 signaling. *Science* 2007;316:1039–43.
 6. Hsieh AC, Moasser MM. Targeting HER proteins in cancer therapy and the role of the non-target HER3. *Br J Cancer* 2007;97:453–7.
 7. Engelman JA, Cantley LC. The role of the ErbB family members in non-small cell lung cancers sensitive to epidermal growth factor receptor kinase inhibitors. *Clin Cancer Res* 2006;12:4372–6s.
 8. Ritter CA, Perez-Torres M, Rinehart C, et al. Human breast cancer cells selected for resistance to trastuzumab *in vivo* overexpress epidermal growth factor receptor and ErbB ligands and remain dependent on the ErbB receptor network. *Clin Cancer Res* 2007;13:4909.
 9. Sergina NV, Rausch M, Wang D, et al. Escape from HER-family tyrosine kinase inhibitor therapy by the kinase-inactive HER3. *Nature* 2007;445:437–41.
 10. Zhou BB, Peyton M, He B, et al. Targeting ADAM-mediated ligand cleavage to inhibit HER3 and EGFR pathways in non-small cell lung cancer. *Cancer Cell* 2006;10:39–50.
 11. Sierke SL, Cheng K, Kim HH, Koland JG. Biochemical characterization of the protein tyrosine kinase homology domain of the ErbB3 (HER3) receptor protein. *Biochem J* 1997;322:757–63.
 12. Li D, Shimamura T, Ji H, et al. Bronchial and peripheral murine lung carcinomas induced by T790M-L858R mutant EGFR respond to HKI-272 and rapamycin combination therapy. *Cancer Cell* 2007;12:81–93.
 13. Ben-Hur A, Ong CS, Sonnenburg S, Scholkopf B, Ratsch G. Support vector machines and kernels for computational biology. *PLoS Comput Biol* 2008;4:e1000173.
 14. Vapnik V. The nature of statistical learning theory. Springer; 1999.
 15. Schoeberl B, Pace EA, Fitzgerald JB, et al. Therapeutically targeting ErbB3: a key node in ligand-induced activation of the ErbB receptor-PI3K axis. *Sci Signal* 2009;2:ra31.
 16. Frollov A, Schuller K, Tzeng CW, et al. ErbB3 expression and dimerization with EGFR influence pancreatic cancer cell sensitivity to erlotinib. *Cancer Biol Ther* 2007;6:548–54.
 17. Guo A, Villen J, Kornhauser J, et al. Signaling networks assembled by oncogenic EGFR and c-Met. *Proc Natl Acad Sci U S A* 2008;105:692–7.
 18. Burnham KP, Anderson DR. Model Selection and Multimodel Inference. 2nd ed. Springer; 2002.
 19. Kobayashi S, Boggon TJ, Dayaram T, et al. EGFR mutation and resistance of non-small-cell lung cancer to gefitinib. *N Engl J Med* 2005;352:786–92.
 20. Pao W, Miller VA, Politi KA, et al. Acquired resistance of lung adenocarcinomas to gefitinib or erlotinib is associated with a second mutation in the EGFR kinase domain. *PLoS Med* 2005;2:e73.
 21. Kim HH, Sierke SL, Koland JG. Epidermal growth factor-dependent association of phosphatidylinositol 3-kinase with the erbB3 gene product. *J Biol Chem* 1994;269:24747–55.
 22. Soltoff SP, Carraway KL III, Prigent SA, Gullick WG, Cantley LC. ErbB3 is involved in activation of phosphatidylinositol 3-kinase by epidermal growth factor. *Mol Cell Biol* 1994;14:3550–8.
 23. Wang SE, Xiang B, Guix M, et al. Transforming growth factor β engages TACE and ErbB3 to activate phosphatidylinositol-3 kinase/Akt in ErbB2-overexpressing breast cancer and desensitizes cells to trastuzumab. *Mol Cell Biol* 2008;28:5605–20.
 24. Montero JC, Rodriguez-Barrueco R, Ocana A, Diaz-Rodriguez E, Esparis-Ogando A, Pandiella A. Neuregulins and cancer. *Clin Cancer Res* 2008;14:3237–41.
 25. Li D, Ambrogio L, Shimamura T, et al. BIBW2992, an irreversible EGFR/HER2 inhibitor highly effective in preclinical lung cancer models. *Oncogene* 2008;27:4702–11.

Cancer Research

The Journal of Cancer Research (1916-1930) | The American Journal of Cancer (1931-1940)

An ErbB3 Antibody, MM-121, Is Active in Cancers with Ligand-Dependent Activation

Birgit Schoeberl, Anthony C. Faber, Danan Li, et al.

Cancer Res 2010;70:2485-2494. Published OnlineFirst March 9, 2010.

Updated version	Access the most recent version of this article at: doi: 10.1158/0008-5472.CAN-09-3145
Supplementary Material	Access the most recent supplemental material at: http://cancerres.aacrjournals.org/content/suppl/2010/03/08/0008-5472.CAN-09-3145.DC1

Cited articles	This article cites 23 articles, 12 of which you can access for free at: http://cancerres.aacrjournals.org/content/70/6/2485.full#ref-list-1
Citing articles	This article has been cited by 39 HighWire-hosted articles. Access the articles at: http://cancerres.aacrjournals.org/content/70/6/2485.full#related-urls

E-mail alerts	Sign up to receive free email-alerts related to this article or journal.
Reprints and Subscriptions	To order reprints of this article or to subscribe to the journal, contact the AACR Publications Department at pubs@aacr.org .
Permissions	To request permission to re-use all or part of this article, use this link http://cancerres.aacrjournals.org/content/70/6/2485 . Click on "Request Permissions" which will take you to the Copyright Clearance Center's (CCC) Rightslink site.